Romanian Reports in Physics, Vol. 67, No. 2, P. 547–563, 2015

IDEAS IN FUSION PLASMA PHYSICS AND TURBULENCE*

B. WEYSSOW[1], M. NEGREA[2], G. STEINBRECHER[2], I. PETRISOR[2], D. CONSTANTINESCU[3], N. POMETESCU[2], M. VLAD[4], F. SPINEANU[4]

[1] Université Libre de Bruxelles, Association EURATOM-Belgian State for Fusion, Campus Plaine CP 231, Bvd du Triomphe, B-1050 Brussels, Belgium, E-mail: bweyssow@ulb.ac.be
[2] University of Craiova, Association EURATOM-MEdC, Department of Physics, Romania
[3]University of Craiova, Department of Applied Mathematics, Association Euratom-MEdC, Romania
[4] National Institute for Laser, Plasma and Radiation Physics, Association Euratom-MEdC, P.O.Box MG-36, Magurele, Bucharest, Romania

Received July 29, 2013

Abstract. Some developments in fundamental theory of stochasticity and turbulence in magnetically confined fusion plasmas relevant to ITER and to the future European fusion power plant DEMO are discussed.

Key words: magnetically confined fusion plasmas, stochasticity, turbulence.

1. INTRODUCTION

Many interesting developments useful to study fusion plasmas have occurred in the recent years but important basic physics related problems remain to be solved such as the L-H transition and the control of the so-called Edge Localized Modes (ELM's) to give but two examples. An overview of the so-called BFR (Belgian-France-Romania research entity) contributions to this physics is provided in relation to works in progress of interest to ITER and DEMO.

1.1. EUROPEAN CONTRIBUTION TO THE PHYSICS OF MAGNETICALLY CONTROLLED FUSION PLASMAS

The group BFR is an agreement between the Belgian, French and Romanian Euratom-Fusion Associations active in basic research in the area of stochasticity and turbulence. The membership evolved in time according to the subject analyzed but the core of it is the physics group at CEA Cadarache, the fusion research unit at ULB, the Physics Department of University of Craiova, and the fusion research

* Paper presented at the 16th International Conference on Plasma Physics and Applications, June 20–25, 2013, Magurele, Bucharest, Romania.

unit at the Institute for Laser Physics at Magurele. The existence of the BFR group is intimately related to the structure of the fusion research in Europe. Today's organization of the EU laboratories activities is based on three structures namely Fusion for Energy (F4E) which delivers the European contribution to the construction of ITER whose objective is to verify the scientific and technical feasibility of thermonuclear fusion as a new source of energy and to prepare the European power plant DEMO, EFDA dealing with specific collaborative activities in the physics and technology of ITER as well as the use of the tokamak JT-60SA in Japan, and the European Commission.

In this framework, the specificity of the BFR group is to deal with physics problems using analytical approaches so as to avoid whenever possible the use of large computers. Examples will be given below. It will be shown that the selected problems are generally directly relevant to the priority list of ITER physics problems in need for a solution, or are intended to shed lights on new difficulties related to power plants such as DEMO.

1.2. EXPERIMENTS

Let us recall in few words the basics of the tokamak physics. In strong constant magnetic fields, the charges particles (ions and electrons) have a motion composed of a gyration around a magnetic field line and a free (longitudinal) motion along it. The neglect of the gyration leads to the so-called guiding centre dynamics. In absence of toroidal current, the Tokamak geometry is build such as to have field lines forming closed loops (toroidal direction). This defines the confinement of the charged particles. At first sight, an electrical current flowing along the closed loops does not change much the picture as far as confinement is concerned. However, in terms of magnetic geometry, a new feature is introduced. Indeed, the electrical current produces a poloidal magnetic field which, added to the toroidal magnetic field, induces a twisting of the magnetic field lines. Looking at the return points in a plane perpendicular to the loops (a toroidal cross section), a field line will in general not return exactly to its departing position but will define a closed loop due to the hamiltonian character of the dynamics. In fact, the field lines, some of which have a finite length while others have infinite length, define a system of nested magnetic surfaces. The seemingly perfect confinement is in fact not so due to the curvature and gradient of the magnetic field responsible for slow drifts of the charged particles across the magnetic surfaces. In reality this loss of total confinement is needed to remove the Helium ash produced by the fusion reactions in the Deuterium-Tritium plasma. The achievements in Tokamak physics since the 60^{th} are depicted in Fig. 1.1 taken from [1] and showing the confinement time as a function of the ion central temperature (*i.e.* the Lawson criteria). The most recent tokamaks are operating in the vicinity of the break-even curve signifying that losses equate the injected power. Iter will operate in the self-ignition region where alpha power replaces the injected power in sustaining the nuclear reactions.

The evaluation of the confinement time relies on a detailed study of the transport properties of the plasma. In the strong constant magnetic field picture, the transport properties are similar to those of a classical gas. In a Tokamak, the magnetic coils are denser near the symmetry axis of the machine than at a radial distance: the toroidal magnetic field is strongest near the axis. By law of conservation of momentum and energy, a charged particle will be repelled from regions of stronger magnetic field. In a Tokamak, this ends-up having the so-called banana trajectories which are periodic trajectories with poloidal and toroidal excursions less than 2pi and finite radial excursion.

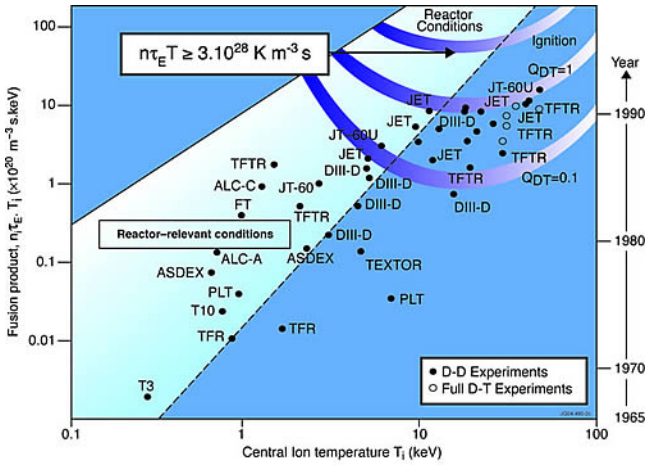

Fig. 1.1 – The improvement in Tokamak confinement time and ion central temperature (*i.e.* the Lawson criteria) for various since the 60th [1].

These trajectories are responsible for a coupling of the transport in the periodic directions (toroidal and poloidal) with the radial direction. Hence, the transport theory applicable to Tokamaks is the so-called neo-classical transport theory and not the too simple classical transport theory. Other important geometrical factors such as the presence of an X-point in the toroidal cross section of the tokamak are also incorporated in the neo-classical transport theory. The X-point (sometimes two X-points) is needed to facilitate the pumping out of the (Helium ash contaminated) edge plasma. It is to remark that the legs going out of the X-point are reaching solid surface named the divertor which therefore has to be resilient to strong particle flux including neutron flux, and strong heat flux besides high temperatures. The final geometry of the Tokamak is depicted in Fig. 1.2 from [2].

Two additional features, further perturbing the confinement of the charge particles, namely, the stochasticity of the magnetic geometry and the turbulence also affect the transport properties of a Tokamak. In many publications, calculations and comparisons with experiments take the neoclassical transport as reference value on top of which one finds the strong influence of the turbulence.

1.3. HIGH CONFINEMENT REGIME AND PLASMA WALL

A transition to a high confinement regime (H-mode as opposed to the L-mode) has been obtained in 1980 on the Tokamak Asdex while injecting additional power to the plasma by ways of electron cyclotron waves. In this new regime, the radial variations of the temperature and density assume very different shape as compared to that of the L-mode. Indeed, very strong gradients at the external edge of the plasma are observed (Fig. 1.3). The steep gradient region is usually named "pedestal". It is believed that the top of the pedestal is determined by the presence of a transport barrier which in simple models takes the form of a Kolmogorov-Arnold-Moser invariant curve (KAM) in a sea of stochastic field lines (this topic will be discussed below) or in more detailed studies the same effect translated at the charges particles level.

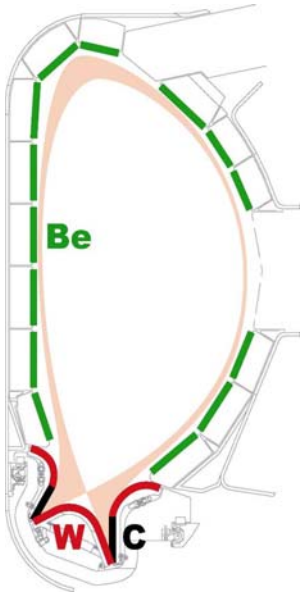

Fig. 1.2 – Geometry of the Tokamak in this case with a single X-point at the bottom of the machine. The divertor in made of tungsten (except for some carbon tiles) as opposed to the wall made of Beryllium in JET Tokamak in the UK and in ITER [2].

This translation is possible as the magnetic field line dynamics is the zero's order of the charged particle dynamics by virtue of the guiding centre transformation.

The main consequence of the H-mode on plasma behavior is the appearance of periodic ejection of strong heat pulses from the plasma which impact negatively on the solid walls and the divertor as shown in Fig. 1.4 (see [4]). These heat pulses are MHD events named Edge Localized modes (ELM's).

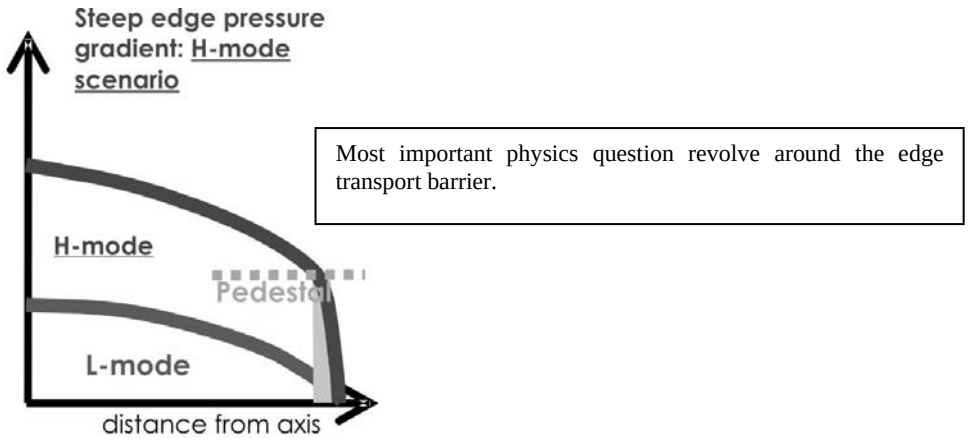

Fig. 1.3 – Radial profiles of the density and temperature in L and H modes in a Tokamak [3].

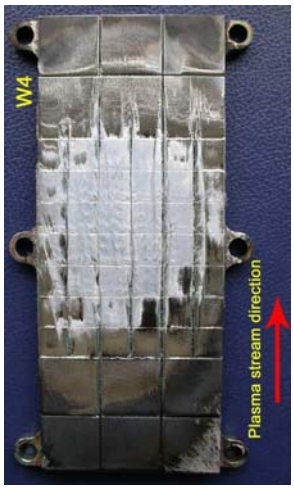

Fig. 1.4 – Modeling of the damage on a tile by the ELM's. The heat pulse experiments consisting of 100 pulses at 0.5, 1.0, 1.5 MJ/m^2 and duration D_t = 500 ms (two higher levels beyond melting of W and sublimation of C) are carried out in TRINITI plasma guns with CFC and W targets [4].

2. RESONANT MAGNETIC PERTURBATIONS

To avoid material destruction, some sort of ELM control or mitigation is necessary. It is thought that ELM's can be controlled by modifying in an appropriate way the confining magnetic field. In general, there are good reasons to deal in plasma theories with magnetic perturbations for they are unavoidable, due for

instance to the finite number of coils, or are produced by MHD instabilities, or are external injected such as in the case of resonance magnetic perturbation (RMP).

As an introduction to the subject, we discuss the Tokamap concept as it was presented by Balescu, Vlad and Spineanu in [5]. The Tokamap is a mapping that describes the return points of the field lines in a toroidal section of the Tokamak. As explained above, in absence of magnetic perturbations, the return points align to form a closed curve demonstrating the existence of nested magnetic surfaces. The tokamap gives a new position y_{n+1}, x_{n+1} of a field line starting at position y_n, x_n where *x* represents the poloidal angle and *y* the radial position in the toroidal cross section:

$$\begin{aligned} y_{n+1} &= \frac{1}{2}\left\{ P\left(x_n, y_n\right) + \sqrt{\left[P\left(x_n, y_n\right)\right]^2 + 4y_n} \right\}, \\ x_{n+1} &= x_n + \iota\left(y_{n+1}\right) - \frac{k}{\left(2\pi\right)^2} \frac{1}{\left(1+y_{n+1}\right)^2} \cos\left(2\pi x_n\right), \end{aligned} \tag{1}$$

where $P\left(x, y\right) = y - 1 - \frac{k}{2\pi}\sin\left(2\pi x\right)$. The model is constructed such as to have a single magnetic axis, and the regular displacement of the return points (sign of the existence of magnetic surface) in absence of any perturbation. This displacement is determined by the function iota which mimics the safety factor profile in the Tokamak: $\iota\left(y\right) = \frac{\iota_0}{4}\left(2-y\right)\left(2-2y+y^2\right)$. The perturbation is periodic in the poloidal angle and its amplitude is controlled by the parameter *k*.

The tokamap received much attention by the BFR group and J. Misguich in particular (see *e.g.* [6]). The structure of the phase space of the Tokamap is shown in Fig. 2.1a in the case of a strong perturbation and the Lyapounov exponents (the exponent determining the divergence of nearby field lines) are shown in Fig. 2.1b and Fig. 2.1c, calculated for a large set of field lines [7]. Despite the simplicity of the model, the obtained dynamics is extremely complex as exemplified by the Lyapounov exponents calculated in Fig. 4c for the small green box region of the top of Fig. 4b. Interestingly enough, by modifying the ι-profile replacing the monotonous function by a function with segments of negative and positive slopes, it is possible to generate magnetic barriers in well defined radial positions (near the minimum of the q-profile). To get a better link with the experiments, one perhaps needs two additional results i) a particle transport barrier is formed when a magnetic barrier is present (using a particle map) and ii) to demonstrate the barrier determines the top of the pedestal.

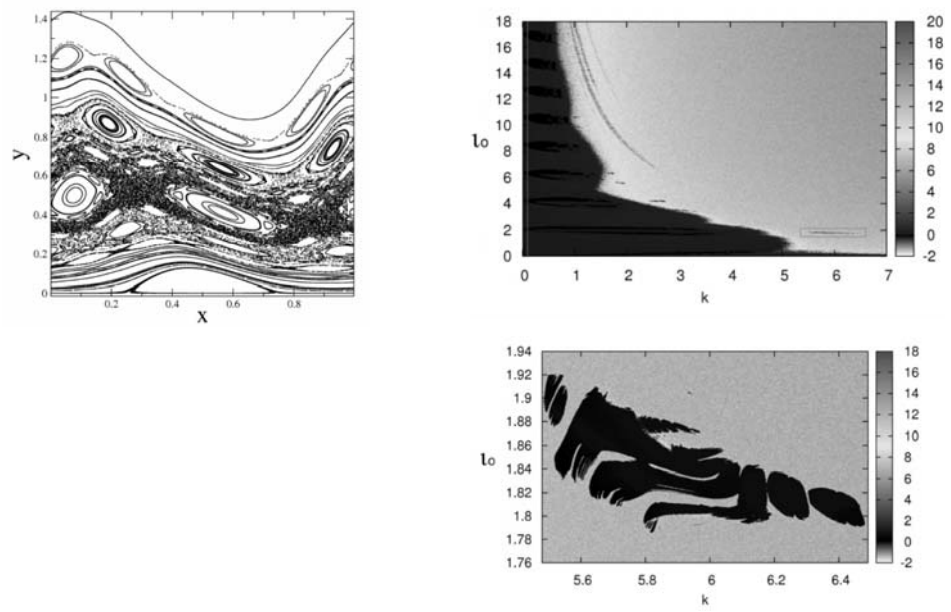

Fig. 2.1 – Phase space portrait of the Tokamap in the case of a strong perturbation (a – left), and Lyapounov exponents calculated for various safety factor values on the magnetic axis and various values of the perturbation amplitude (b – right top). In c are (right bottom) showing the details of the Lyapounov exponents corresponding to the small green area of b. Lowest values of the Lyapounov exponents are in the blue-black colors. Plots are from [7].

The "resonance magnetic perturbation" is an experimental set-up (Fig. 2.2) which on TEXTOR takes the form of multiple sets of coils placed in the inner side of the Tokamak. The objective is to modify the edge properties of the plasma by changing the underlying structure of the magnetic field.

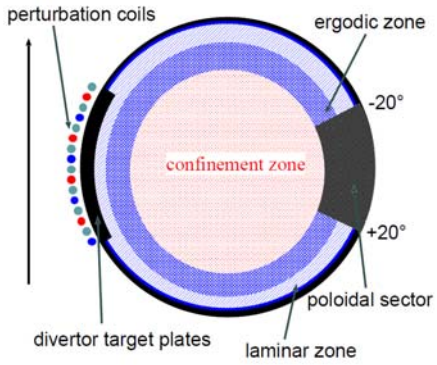

Fig. 2.2 – TEXTOR equipped with sets of resonance magnetic perturbation coils on the inner side of the Tokamak. In this experiment by switching on/off different sets of coils it is possible to induce time periodic perturbations acting on different rational values of the safety factor [8].

The results are best seen on the D_α signal as shown in Fig. 2.3 from [9].

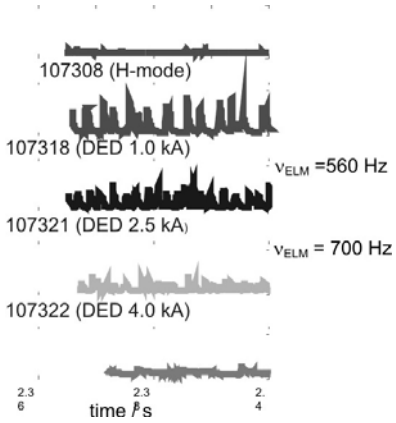

Fig. 2.3 – The $D\alpha$ signal for different RMP frequencies and amplitudes in the TEXTOR experiment [9]. A control of the ELM's amplitude is achieved by increasing the amplitude of the perturbation. However, the ELM's react by adapting their frequencies so that globally the heat flux transported by the ELM's is not much reduced.

Concerning the magnetic topology, one can again use the Tokamap but now using a different construction of the perturbation term (see *e.g.* [10]). The main drawback of this approach is that the magnetic field is not fully consistent with the presence of the plasma so that penetration of the field is not perfectly well evaluated. Despite of this, a good correspondence is observed between the magnetic field structure generated using the mathematical model and the experimental one. This is demonstrated by comparing Fig. 2.4 with Fig 2.5 below. The first one shows the connection length between an initial point taken inside and going to the edge of the Tokamak. The shortest values are shown in blue and occupy a large area embraced by two "arm" which have much longer connection length. The arms are oriented towards the edge and are directing towards an edge region at higher temperature.

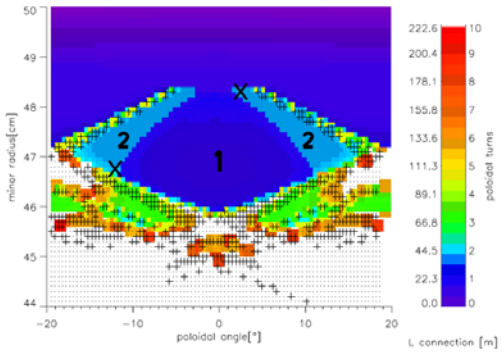

Fig. 2.4 – Connection length (from initial position to target plate [8]).

In order to include plasma in the description a system of MHD equations has been produced [8]:

$$\begin{aligned}
&\nabla_{\perp}\left(D_{\perp}\nabla_{\perp}n\right)+D_{//}\left(nv_{//}\right)=0,\\
&\nabla_{\perp}\left(\chi_{\perp}n\nabla_{\perp}T+5TD_{\perp}\nabla_{\perp}n\right)+\nabla_{//}\left(5nv_{//}T-\kappa\nabla_{//}T\right)=0,\\
&\nabla_{//}\left(m_{p}nv_{//}^{2}+2nT\right)=0.
\end{aligned} \tag{2}$$

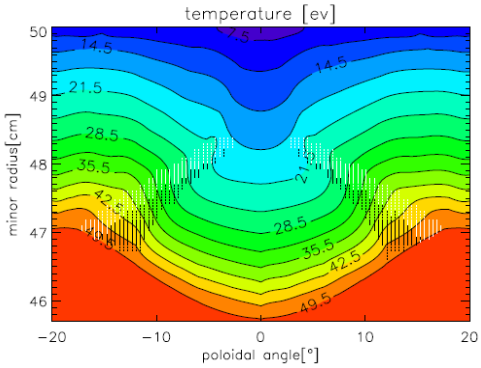

Fig. 2.5 – Plasma temperature near the edge from MHD calculations using Eq. (2) reproduces the two “arms”. The prolongation of these features to the edge (top of the figure) leads zone at higher temperature than the rest of the edge region.

3. MORE ON ELM’S

Various alternative methods to the RMP have been developed to stabilize the ELM’s. An example is by moving the whole plasma vertically very quickly. Another method, analyzed by an extension of the method described in this section, is by injecting pellets inside the plasma [11]. To understand what is going on while using these methods one would be interested in an analysis providing a trajectory in some kind of parameter space allowing the system to move from one state (ELM state) to a quiescent state (Elm free state). Such analysis is in essence what has been done in Ref. [11] and in Ref. [12].

The edge localized modes are periodic structures thought to be related to displacement of the magnetic field ξ linked to pressure gradient dynamics p_n'. A minimal model produced in has two parameters η and δ [11]:

$$\begin{aligned}
&\frac{\mathrm{d}^2}{\mathrm{d}t_n^2}\xi_n=\left(p_n'-1\right)\ \xi_n-\delta\frac{\mathrm{d}}{\mathrm{d}t_n}\xi_n,\\
&\frac{\mathrm{d}}{\mathrm{d}t_n}p_n'=\eta\ \left(h-p_n'-\beta\xi_n^2p_n'\right),
\end{aligned} \tag{3}$$

where $\beta = \chi_{anom} / \chi_0$. Studying this system using ASDEX-Upgrade parameters leads to a parameter space sketched in Fig. 3.1. The model seems to correctly reproduce the domain of ELM's relevant to the ASDEX-Upgrade Tokamak but leaves little possibility to act on the system to bring it into a quiescent regime. Therefore, from this parameter plot one sees little possibility to control the ELM's due to restricted experimental parameter space. A similar analytical approach is followed in [12] where plasma rotation is also considered. That plasma is in rotation and at which speed is an important issue for ITER since as we shall see in the present case, rotation has a strong impact on the plasma dynamics. Rotation is easily induced by means of neutral beam injection. Intrinsic rotation is discussed when no external source of plasma rotation is applied or when sources exactly compensate as when one of two neutral beams is co-current, the other contra-current.

In Fig. 3.2, both ψ and a_N represents the radial direction. Fig. 3.2a shows the pressure gradient as a function of the radial position inside the plasma.

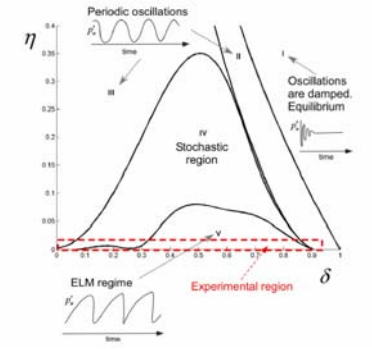

Fig. 3.1 – Sketch of the parameter space and the various types of dynamics encountered by varying the available parameters η and δ .

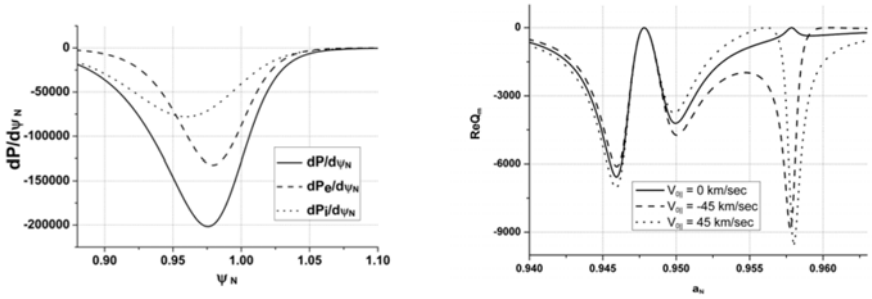

Fig. 3.2 – Pressure gradient profile using DIII-D parameters (a-left), profile of the function Q_m (b-right) for various plasma rotation speed [12].

Looking into the details of the equations, and in particular to a contribution denoted Q_m to the pressure gradient, one observes, as depicted in Fig. 3.2b, that plasma rotation induces a resonant perturbation at the edge of the plasma.

Besides the important impact rotation has on the plasma dynamics we now see that the parameter space must be modified to include rotation which might imply new possibilities of controlling the ELM's.

To corroborate the simplified analysis, MHD simulations using the numerical code JOREK are now possible. Indeed, Fig. 3.3 from [13] shows the plasma temperature (left) and density profiles (right) during an ELM in ITER, showing conductive losses in the perturbed magnetic field (left) and expulsion of plasma filaments (right).

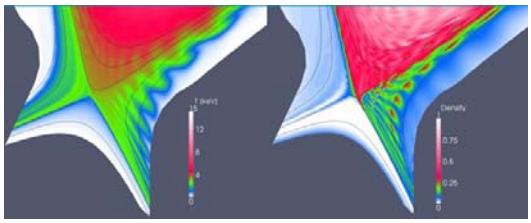

Fig. 3.3 – JOREK simulations of the divertor region below the X-point during an edge localized mode (ELM) [13].

4. ON PLASMA TURBULENCE

To demonstrate the complicated structures arising due to turbulent fields we present a plot (Fig. 4.1) of an Ion Temperature Gradient (ITG) non-linear simulation using a global/full-f with self consistent neoclassical flows [14]. The ITG is one of the modes related to drift wave turbulence. The separatrix is the magnetic surface passing through the X-point and going to the divertor while the pedestal top is where, as explained before, one expects to find a transport barrier. As shown in the figure, the ITG turbulence does not go much beyond the separatrix towards the edge and seems rather to propagate inwardly.

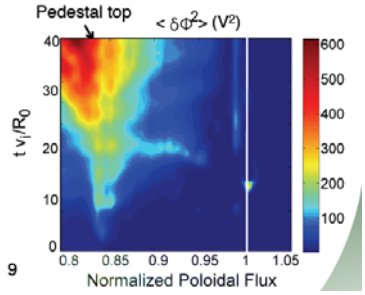

Fig. 4.1 – ITG non-linear simulation using a global/full-f GK from [14] showing the fluctuation pattern evolving in time as a function of the radial position. The white line corresponds to the position of the separatrix.

While the plot Fig. 4.1 does not provide the possibility to look at all the statistical details one can infer that non classical particle dynamics may occur such as sub-diffusion (due to trapping of the charged particles for example) or superdiffusion (due to ballistic motion) as well as non Gaussian transport. Outside the separatrix, closer to the edge in the region named "Scrape off layer" (SOL), measurements of the particle transport are easier due to lower temperatures (for a recent numerical simulation see [15]). It is indeed observed in the SOL that non Gaussian effects (heavy tails in the distribution function) play an important role probably due to the variety of connection lengths to the Tokamak wall and due to the Kelvin-Helmholtz instability.

Models have been developed dealing either with the bursty behavior or with the heavy tails of the distributions. Included, are the methods based on the Langevin equations for charged particles in stochastic fields as considered by the BFR group. An interesting case is when the noise is produced by a combination of fractional Brownian motions introducing self-similarity [16]. Indeed, in this case, it is possible to have at once, a bursty behavior and heavy tails. The problem of non-gaussianity in the SOL analyzed with the "Random Linear Amplification Model" is giving $\left\langle |r(t)|^p \right\rangle \propto \exp[(p-\beta)t]$ that is $p-\beta = \lim_{t\to\infty} \log\left|\left\langle r(t)^p \right\rangle\right| / t$ instead of the usual anomalous result from sub or super diffusion calculations $\left\langle |r(t)|^p \right\rangle \propto t^{\zeta_p}$ or $\zeta_p = \lim_{t\to\infty} \log\left|\left\langle r(t)^p \right\rangle\right| / \log(t)$.

While this model is compatible with many physical observations, its properties could also be of some interest in the analysis of the L-H transition as indeed correlations in the radial electric field may play an important role. Thus, the use of the random amplification model as a source of stochasticity in the random L-H transition model [17] (which at least couple a change of the DC radial electric field, becoming in general strongly negative at the L-H transition, to the strongly reduced level of turbulence in the H-mode) might bring some interesting results and perhaps explain why it is presently not possible to simulate the L-H transition with Gyrokinetic codes.

This brief discussion of the L-H transition brings in another question mark in the ITER related physics. It concerns the role of drift waves and zonal flow in plasma rotation. Zonal flows are related to the transport barrier in the H-mode which results from a shear flow in the poloidal direction (perpendicular to the magnetic field and the gradients). This flow carries no uniformly the drift wave structures which eventually break into smaller structures. The drift wave turbulence could be the source for this drift wave (poloidal) zonal flow. The existence of the zonal flow has been demonstrated experimentally by identifying radial electric field oscillations before and after LH transition, correlated to Reynolds Stress [18]. The theory of zonal flow, still in development, received some attention by the BFR group. An advanced analysis [19] consists in solving a Wave Kinetic Equation (as discussed by many authors) using the "Decorrelation Trajectory Method" first

published in [20]. The later method received much attention by the BFR group and others. A wave kinetic equation (WKE) defines the evolution of an action density $N(k) \approx e(k)/\omega_d(k)$ ration of the drift wave energy $e(k)$ to the drift wave frequency $\omega_d = k_y V_* / \left(1+\rho_s^2 k^2\right)$, where $V_* = \rho_s c_s / L_n$ is the electron diamagnetic velocity, ρ_s is the electron Larmor radius, c_s is the sound speed, L_n is the density gradient length. The action density is a function of space, of the wave vector and of time. The WKE is Hamiltonian with canonical variables (x,k) and reads:

$$\partial_t N = L_W N \equiv [H, N]. \tag{4}$$

The Hamiltonian $H(x,k,t) = \omega_d(k) + k \cdot V(x,t)$ for the drift wave is composed of two contributions namely the drift wave frequency $\omega_d(k)$ and the product $k \cdot V$ where $V = (\varepsilon c / B)(e_z \times \nabla \phi)$ is the long range part of the $E \times B$ guiding center drift velocity. An overview of the method proposed in [10] is now provided. The action density is composed of a non fluctuating part $n(x,k,t)$, corresponding to the zonal flow, and of a fluctuating part $\delta N(x,k,t)$: $N(x,k,t) = n(x,k,t) + \delta N(x,k,t)$. The WKE separates out into two equations, the one for the fluctuating part of the action density is integrated and the solution introduced into the remaining equation. The result is as follows:

$$\partial_t n(x,k,t) + V^g(k) \cdot \partial_x n(x,k,t) = \int_0^t \mathrm{d}t_1 \left(\sum_{a,b=(x,k)} \partial_a \cdot L^{AB} \cdot \partial_b \right) n(x,k,t_1), \tag{5}$$

where the L^{AB}, with $A,B = (X,K)$, is a Lagrangian correlation tensor $L^{AB}_{r|s}(t-t_1) = \left\langle \dot{A}_r[x,k,t]\, \dot{B}_s[x(t_1),k(t_1),t_1] \right\rangle$. The dot represents the total time derivative so that the quantities involved are the drift wave velocity $\dot{X}$ and the wave vector velocity $\dot{K}$ in the (x,k) phase space. The diffusion coefficients (transport coefficient) are easily derived from the Lagrangian: $D^{KK}_{r|s}(t) = \int_0^t \mathrm{d}t_1 L^{KK}_{r|s}(t_1)$. We now introduce succinctly the concept of "Decorrelation trajectory method" [20]. The first step is to extract the characteristics of the WKE typically of the form:

$$\begin{aligned}\frac{\mathrm{d}x(\theta)}{\mathrm{d}\theta} &= K_d v^g\left[k(\theta)\right] + Kv\left[x(\theta),\theta\right],\ x(0)=0\\ \frac{\mathrm{d}k(\theta)}{\mathrm{d}\theta} &= Kw\left[x(\theta),k(\theta),\theta\right],\ k(0)=k^0.\end{aligned} \tag{6}$$

The second step consists in selecting a set of initial conditions (sub-ensemble)

$$S:\phi(0,0)=\phi^0,\ \ v_r(0,0)=v_r^0,\ \ -k_s^0\nabla_r v_s(0,0)=w_r^0.$$

The third step is to introduce a probability distribution function P_0 for these initial conditions. It then follows that for example

$$L_{x|x}^{KK}(\theta)=\int \mathrm{d}\phi^0\mathrm{d}v^0\mathrm{d}w^0 P_0\left(\phi^0,v^0,w^0\right)w_x^0\left\langle w_x\left[x(\theta),k(\theta),\theta\right]\right\rangle^S. \tag{7}$$

The solution consists now in solving the characteristics equations in the sub-ensemble, then use the trajectories in Eq. (7) and finally to derive the diffusion coefficient. This program has been realized in [19] indeed demonstrating a diffusion in k-space of the Drift Wave structure. Gyrokinetic simulations are showing the similar results, of the type shown in Fig. 4.2 from [21].

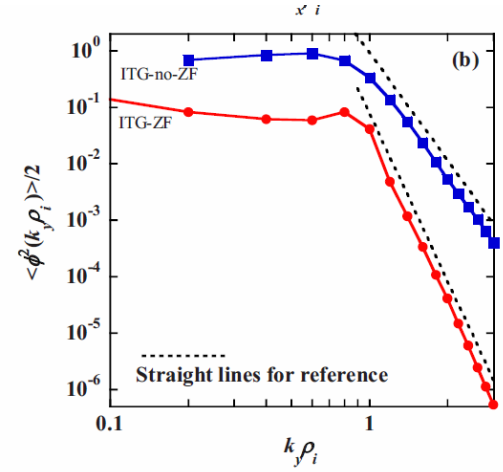

Fig. 4.2 – Comparison of the spectrum of the drift wave turbulence with and without zonal flow [21].

Most recently the question arose on how to describe the drift wave turbulence, essentially 2D in the toroidal cross section when it is modified by parallel dynamics along the magnetic field. A model equations was proposed in [22] coupling the drift wave to the ion acoustic wave. This gives to study:

$$\begin{aligned}
&\frac{\partial}{\partial t}\left(\nabla_{\perp}^{2}\phi-\phi\right)+\hat{z}\times\nabla\phi\cdot\nabla\nabla_{\perp}^{2}\phi+\left(\frac{\partial}{\partial r}\ln n_{0}\right)\frac{\partial}{\partial y}\phi= \\
&\quad=\tilde{f}+\mu\nabla^{2}\left(\nabla_{\perp}^{2}\phi-\phi\right)+\nabla_{//}u_{//}, \\
&\left(\frac{\partial}{\partial t}+\hat{z}\times\nabla\phi\cdot\nabla\right)u_{//}=-\nabla_{//}\phi.
\end{aligned} \tag{8}$$

Is the method based on the wave kinetic equation (WKE) together with decorrelation trajectory method (DCT) still working? We have to solve the system

$$\begin{aligned}
&\frac{\partial}{\partial t}\phi_{k}+\mathrm{i}\omega_{k}^{\phi}\phi_{k}+\int\mathrm{d}^{3}pL_{p,k-p}^{\phi}\phi_{p}\phi_{k-p}=-\mathrm{i}\omega_{k//}^{\phi}u_{//k}, \\
&\frac{\partial}{\partial t}u_{//k}+\int\mathrm{d}^{3}pL_{p,k-p}^{u//}\phi_{p}u_{//k-p}=-\mathrm{i}\omega_{k//}^{u//}\phi_{k},
\end{aligned} \tag{9}$$

where $L_{k1,k2}^{\phi}=-\frac{c}{B}\frac{b\cdot k_{1}\times k_{2}}{1+\left(k_{1}+k_{2}\right)^{2}\rho_{x}^{2}}\left(1+k_{2}^{2}\rho_{s}^{2}\right)$ and $L_{k1,k2}^{u//}=-\frac{c}{B}b\cdot k_{1}\times k_{2}$.

Similarly to [23] but with coupled equations, large scale separation in the turbulence is assumed. The idea is to remove the small scales (large k, high frequency; superscript >), keeping larger scales (small k, low frequency; superscript <) and mean flow then to write the correlations of the stochastic quantities (the potential and the parallel velocity):

$$I_{k}^{AB}\left(x,t\right)\equiv\int\mathrm{d}^{3}q\ \left\langle A_{k}^{>}\quad B_{-k+q}^{>}\right\rangle\ \exp\left(\mathrm{i}q\cdot x\right). \tag{10}$$

We then get for example

$$\begin{aligned}
&\frac{\partial}{\partial t}I_{k}^{\phi\phi}\left(x,t\right)+\frac{\partial\omega_{k}^{\phi}}{\partial k}\cdot\frac{\partial I_{k}^{\phi\phi}}{\partial x}-2I_{k}^{\phi\phi}\left(x,t\right)\ \frac{1}{1+k^{2}\rho_{s}^{2}}\ \frac{\partial\left(1+k^{2}\rho_{s}^{2}\right)}{\partial k}\cdot\frac{\partial\left(k\cdot V_{0}^{<}\left(x\right)\right)}{\partial x}- \\
&\quad-\frac{\partial I_{k}^{\phi\phi}}{\partial k}\cdot\frac{\partial\left(k\cdot V_{0}^{<}\left(x\right)\right)}{\partial x}+\frac{\partial I_{k}^{\phi\phi}}{\partial x}\cdot\frac{\partial\left(k\cdot V_{0}^{<}\left(x\right)\right)}{\partial k}=0.
\end{aligned} \tag{11}$$

In total, four equations similar to the above one are produced. To analyze them, the first step is to verify that the Wave Kinetic formalism works fine. The second step is the extended DCT method. Concerning the first step, the equations we have to analyze can be cast in the generic form

$$\frac{\partial U}{\partial t}+\sum_{i=1}^{n}A_{i}\frac{\partial U}{\partial x_{i}}=0\quad t>0, \tag{12}$$

where x_i and t are the independent variables. The coefficients A_i read symbolically in our case (the first term in the parenthesis corresponds to $\partial_x U$, the second to $\partial_k U$):

$$A = \begin{Bmatrix} \{a,0\} & \{d,0\} & 0 & 0 \\ \{e,0\} & 0 & \{c,b\} & 0 \\ 0 & \{0,b\} & \{a,0\} & \{d,0\} \\ 0 & 0 & \{e,0\} & \{c,b\} \end{Bmatrix}. \tag{13}$$

Here, $a = -\partial_x\left(\omega_k^{\phi} + k \cdot V_0^{<}(x)\right)$, $b = \partial_x\left(k \cdot V_0^{<}(x)\right)$, $c = -\partial_k\left(k \cdot V_0^{<}(x)\right)$, $d = -\partial_k\left(\omega_{k//}^{\phi}\right)$, and $e = \partial_k\left(\omega_{k//}^{u//}\right)$. The complications arising in this analysis are as follows. First, the system is made of four coupled WKE of seven independent variables (3 for space, 3 for wave vector, one for time) and on few parameters. The conditions of hyperbolicity needed for defining the total time derivative necessary to express the trajectories in the (k, x) space are available but not trivial. The method of bi-characteristics, usually employed for non turbulent cases, gives a hint on how to define the trajectories needed to develop the DCT method from which the transport analysis should follow. This program has still to be completed.

5. CONCLUSION

Our aim in this presentation has been to make a parallel between the Fusion Program in general and a small subset of fundamental (basic) studies performed under the Contracts of Association–Euratom. Problems in a) MHD activities in plasmas (ELM's and RMP), b) Stochastic processes (Particle dynamics) and c) Kinetic processes (Wave kinetic & DCT) were introduced and additional problems open to further studies are presented. Most of these problems relate indirectly to the development of better methods of controlling MHD and turbulence.

REFERENCES

1. EFDA Organization, http://www.efda.org/2005/12/50-years-of-lawson-criteria/
2. T. Hirai *et al*., Fusion Engineering and Design, **82**, 1839–1845 (2007).
3. Courtesy EFDA organization.
4. A. Loarte, 7th ITPA Divertor and SOL Physics Group, Donghua University, Shanghai, China, 2006.
5. R. Balescu, M. Vlad, F. Spineanu, Phys. Rev. E, **58**, 951–964, 1998; Lecture Notes in Physics, **511**, 241–261 (1998).

6. J. H. Misguich, Physics of Plasmas, **8**, 2132–2138 (2001).
J. H. Misguich *et al.* Plasma Phys. Control. Fusion, **44**, L29 (2002).
7. A. Celestino *et al*., Dynamic Days South America, São José dos Campos – (SP, Brazil), July 26–30, 2010.
8. T. Eich *et al*., Nuclear Fusion, **40**, 1757–1772, 2000; Rev. Mod. Phys., **72**, 733–756 (2000).
9. S. Soldatov *et al*., 9th International Reflectometry Workshop (IRW9), Lisbon, Portugal, 4th–6th May, 2009.
10. S. S. Abdoullaev, Physics of Plasmas**, 16**, 030701–030704 (2009).
11. D. Constantinescu, O. Dumbrajs, V. Igochine, K. Lackner, R. Meyer-Spasche, H. Zohm, and ASDEX Upgrade Team, Physics of Plasmas, **18**, 062307 (2011).
12. I. M. Pankratov *et al.*, Problems of atomic science and technology, BAHT, **1**, 23–25 (2011); Problems of atomic science and technology, BAHT, **6**, *82*, 61–63 (2012).
13. G. Huijsmans, AIEA Annual Conference, JW Marriott, Washington DC, Feb. 19–22, 2012.
14. C. S. Chang *et al*., *Large Scale Computing and Storage Requirements for Fusion Energy Sciences*, Aug. 3–4, Washington DC, 2010.
15. P. Ricci *et al.*, Phys. Plasmas, **20**, 010702 (2013).
16. G. Steinbrecher *et al*., Physical Review Letters, **92**, 125003 (2004);
Romanian Journal of Physics, **55**, 1120–1130 (2010).
17. B. Weyssow, 30th EPS Conference on Contr. Fusion and Plasma Phys., St. Petersburg, 7–11 July, ECA; **27A**, P–3.147 (2003);
M. Negrea *et al.*, J. Optoelectronics and Advanced Materials, **10**, 1946–1949 (2008).
18. G. S. Xu *et al.*, Physical Review Letters, **107**, 125001 (2011).
19. R. Balescu, Phys. Rev E., **68**, 046409 (2003);
R Balescu *et al.*, Plasma Phys. Control. Fusion, **47**, 2145 (2005).
20. M. Vlad *et al.*, Physical Review E, **58**, 7359–7368 (1998).
21. J. Li and Y. Kishimoto**,** Physics of Plasmas, **17**, 072304 (2010).
22. L.Wang *et al*., Plasma Phys. Control. Fusion, **54**, 095015 (2012).
23. A. I. Smolyakov and P. H. Diamond, Phys. of Plasmas, **6**, 4410–4413 (1999).